Article

Mechanical Durability of Low Ice Adhesion Polydimethylsiloxane Surfaces

Pablo F. Ibáñez-Ibáñez, Francisco Javier Montes Ruiz-Cabello, Miguel A. Cabrerizo-Vílchez, and Miguel A. Rodríguez-Valverde*

Cite This: *ACS Omega* 2022, 7, 20741−20749
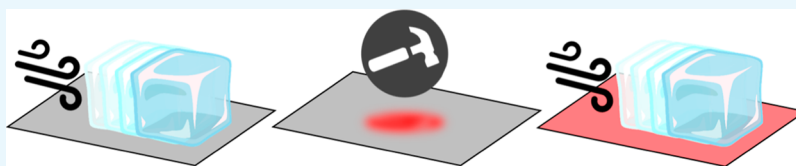
Read Online

| ACCESS | Metrics & More | Article Recommendations | Supporting Information |

ABSTRACT: Elastomeric surfaces and oil-infused elastic surfaces reveal low ice adhesion, in part because of their deformability. However, these soft surfaces might jeopardize their mechanical durability. In this work, we analyzed the mechanical durability of elastic polydimethylsiloxane (PDMS) surfaces with different balances between elasticity and deicing performances. The durability was studied in terms of shear/tensile ice adhesion strength before and after different wear tests. These tests consisted of abrasion/erosion cycles using standard procedures aimed to reproduce different environmental wearing agents. The main objective is to evaluate if our PDMS surfaces can become long-lasting solutions for ice removal in real conditions. We found that our elastic surfaces show excellent durability. After the wear tests, the ice adhesion strength values remained low or even unaltered. Although the oil-infused PDMS surface was the softest one, it presented considerable durability and excellent low ice adhesion, being a promising solution.

1. INTRODUCTION

For designing icephobic materials, an extended assumption is that water-repellent surfaces might show a good anti-icing performance. Due to their poor affinity to water, super-hydrophobic surfaces (SHSs) should avoid or reduce ice accretion. SHSs are able to expel incoming water drops after the impact, so drops may leave the surface before freezing on it.[1−4] In addition, SHS could produce freezing delay and retard frost formation due to the reduced contact area with the drops.[5−8] Moreover, SHS might reduce the ice adhesion, but it was shown that in some cases, due to the interlocking effect (ice anchoring to the surfaces asperities), SHSs do not reduce ice adhesion.[9,10] This is particularly true when ice is formed on the surface under humid conditions, due to frost (or dew) formed between surface asperities.[10−13] This results in a significant reduction of the air trapped within the contact area after water freezing.[11,14,15] More importantly, SHSs show a low durability due to their degradation during ice detachment.[12,13] A more recent alternative approach was the use of slippery liquid-infused porous surfaces (SLIPS) because they also revealed good liquid repellency, delay frost formation, and reduce ice adhesion.[16,17] However, durability is again an issue on SLIPS, whose properties depend on the stability of the top lubricant film, and it could deplete under intensive use.[18] Rykaczewski et al.[19] found that ice formation could displace the oil; this causes an increase in ice adhesion by mechanical interlocking, and surface durability is reduced. Moreover,

SLIPS durability can also be compromised by lubricant evaporation.[20,21] To address this issue, the stability of the lubricant film has been studied and improved to enlarge durability.[21−24]

Even if a given surface was able to reduce ice formation, ice would eventually appear under extreme conditions. Thus, the route can focus on reducing the ice adhesion strength rather than avoiding the ice accretion. A balance between low ice adhesion and durability is getting more attention and needs to be improved, as also stated in a recent review.[25] It is accepted that a surface shows low ice adhesion when the detachment pressure is lower than 100 kPa and super-low ice adhesion for values lower than 10−20 kPa.[26,27] With these former values, ice is spontaneously detached under natural forces such as wind, gravity, or ambient vibrations.

More recently, new surfaces with promising anti-icing performance have emerged. These surfaces are elastomeric, with low ice adhesion strength due to their deformability.[28−30] In addition, some types of elastomeric surfaces combine the properties of SLIPS, such as oil-infused polymer matrix

surfaces.[31,32] This combination improves durability due to their self-repairing properties.[33,34] Moreover, certain elastic surfaces have shown resistance to ice formation−detachment cycles without noticeable increase in ice adhesion strength.[29,33,35] However, surface deformability might rule mechanical durability. In this work, we analyzed the mechanical durability of three elastic polydimethylsiloxane (PDMS) surfaces with very different elastic moduli and low ice adhesion strength. The ice adhesion strength of the surfaces was evaluated in tensile and shear modes, before and after durability tests consisting of abrasion/erosion cycles using standard procedures aimed to emulate different wearing conditions.

2. MATERIALS AND METHODS

2.1. Surface Preparation. The elastomeric surfaces were prepared by using a commercial PDMS Sylgard 184 (DOWSIL). Three types of elastic surfaces were made by using three mixtures. The first mixture was prepared by mixing the cross-linking agent (curing agent) and the silicone base in 1:10 ratio in weight as it is recommended by the manufacturer. The second mixture was prepared by mixing the curing agent-PDMS in 1:1 ratio. The third mixture (oil-infused surfaces) was prepared by a mixture between the curing agent-PDMS in 1:2 ratio. Subsequently, this mixture is again mixed with silicone oil (Sigma-Aldrich 100 cSt) at 50% in weight. This sample will be referred to as 1:2.50%. All mixtures were vigorously stirred and degassed in a vacuum pump for bubble removal (at least 10 min). Then, 7.2 mL of the mixtures was poured over glass slides (76×52 mm²) placed in molds (3D printed with polyethylene terephthalate glycol) to avoid the leaking during the curing process. The entire curing process was conducted in an oven at 60 °C for 24 h. Then, the coated glass surfaces were demolded. Both the PDMS 1:10 and PDMS 1:1 surfaces were sonicated in ethanol, rinsed with ethanol, and later with distillate water. The PDMS 1:2.50% surfaces were simply rinsed with distillate water. The thickness of the final PDMS coating was approximately 2 mm.

Surfaces of PDMS 1:10 with lower thickness were also fabricated following a very similar protocol but pouring less amount (4, 2, or 1 mL) of the PDMS mixtures over the glass slides. These surfaces were employed to examine the relationship between durability and initial surfaces thicknesses.

2.2. Surface Characterization. *2.2.1. Wetting Properties.* The wetting properties of the PDMS surfaces were characterized by two different methods: the tilting plate and the growing-shrinking drop. The tilting plate method[36−38] was used to estimate the sliding angle (SA), the advancing contact angle (ACA), and the receding contact angle (RCA) of the PDMS surfaces as 1:10, 1:1, and 1:2.50%. These measurements were carried out using 70 μL of Milli-Q water drops. In addition, the PDMS 1:10 and PDMS 1:1 surfaces were characterized by means of the growing-shrinking drop method.[39,40] In this method, an initial static drop of 50 μL was grown up to 200 μL at a constant flow rate of 2 μL/s aimed to measure the dynamic ACA. Then, the drop was relaxed for 120 s, and then, a "relaxed" ACA was again measured. Subsequently, the drop volume was decreased down to 50 μL, again at 2 μL/s to measure the dynamic RCA. Then, the drop was again relaxed for 120 s, and the "relaxed" RCA was measured. This complex protocol is motivated by our previous study,[41] in which we found that, for elastic surfaces such as PDMS, the dynamic ACA and RCA may be

overestimated and underestimated, respectively, when they are measured with standard growing-shrinking protocols. To reach a quasi-static state, the flow rate for PDMS surfaces must be really low, which is time consuming. An alternative option is to let the drop relax for some time, which allows it to reach a quasi-static situation.[41] Thus, we proposed to modify the standard growing-shrinking experiment protocol to include a relaxation step that allowed us to measure the quasi-static values of ACA and RCA.

The PDMS surface 1:2.50% was not characterized with the growing-shrinking drop method since these experiments require to drill a hole for water injection-suction from below. With this purpose, it is necessary to use a cutting fluid, which could contaminate the oil-infused surface. For the PDMS surfaces 1:10 and 1:1, the plausible contamination may be mitigated after sonicating each sample in ethanol, but this protocol is not appropriate for oil-infused surfaces.

2.2.2. Elastic Modulus. The elastic moduli of the surfaces were measured by compression using the same method described elsewhere.[41] A 13.00 ± 0.05 mm diameter cylindrical flat metal tip and a dynamometer (IMADA ZTA-200N) coupled to a motorized linear stage (IMADA MH2-500N-FA) compress the surfaces, and the elastic moduli are calculated with the expression $E = (F/A)/(\Delta L/L) = (F/\Delta L)(L/A)$, where L is the film thickness, A is the contact area, and $F/\Delta L$ is the slope of the force versus displacement curve.

2.2.3. Surface Roughness. The surface roughness was characterized using a white light profilometer (PLμ 2300, Sensofar). The scanning area was 285.38×209.62 μm² with a 50× magnification, and the vertical step was fixed to 0.2 μm. At least four runs were taken for each surface. This instrument provides the values of roughness parameters R_a (arithmetic mean roughness) and R_q (root mean squared roughness). Occasionally, the surfaces were also characterized with 20× magnification (694.41×510.09 μm², 0.5 μm step) and 10× magnification (1390×1020 μm², 2 μm step).

2.2.4. Ice Adhesion. An ice block was formed inside a hollow cylinder placed over the surface, filled with Milli-Q water and cooled to −10 °C. Ice adhesion strength was measured with two modes: tensile mode and shear mode. In the tensile mode, the ice block was detached by a force applied perpendicular to the surface, while in the shear mode, the ice block was pulled parallel to the surface (force application point is located at 1.0 ± 0.5 mm from the surface). The peak force measured immediately before the ice detachment is divided by the contact area to obtain the ice adhesion strength (pressure). This area was 76.4 ± 1.9 mm². Further details about ice adhesion measurements can be found elsewhere.[42] A schematic diagram can be found in Supporting Information Section S1.

2.3. Wear by Abrasion. To evaluate the mechanical durability of the PDMS surfaces, abrasion tests were carried out by using the Taber 5750 linear Abraser (Taber Industries). With this setup, an abrader is placed over the surfaces, and it moves back-forward to induce surface damage. The linear motion is produced by a slider-crank mechanism, so the linear speed varies harmonically. The abrader is an aluminum cylinder with nearly 1-inch diameter (25.15 ± 0.05 mm). Sandpapers of different grit numbers were fixed on the cylinder surface to produce different abrasions. The weight of the piece can be altered to increase the abrasion pressure. The stroke length of the back-forward motion and its rate can also be modified. In this work, the stroke length was fixed to 1 in. (25.4 mm) and the rate to 60 cycles/min. Each cycle

corresponds to a back-forward movement. The maximum linear speed of the abrasive piece can be calculated as $S_{Max} = 2\pi r \times V_{Ang}$ where r = stroke length/2, and its average speed as $S_{Avg} = 2 \times$ stroke length $\times V_{Ang}$. In this case, $S_{Max} = 79.80 \pm 0.16$ mm/s and $S_{Avg} = 50.80 \pm 0.10$ mm/s. The abraded area was 11.4 ± 0.1 cm^2. The chosen sandpaper grit was P320 (BUEHLER, average particle diameter 46 μm), and the pressure was fixed to 20.5 kPa. These parameters cause moderate damage on the different surfaces. The abrasion test was conducted up to 4000 cycles. The sandpaper was replaced frequently to ensure that it maintained its properties. After a certain number of abrasion cycles, the surfaces were gently cleaned with a brush and water to remove rests of detached material. The ice adhesion properties and the weight loss (measured by means of a microbalance) were evaluated periodically after a certain number of cycles. The thickness loss of the coatings was estimated from weight loss and abraded area values. The surface roughness after wearing was also measured. Durability was also examined with 5.7 kPa pressure (instead of 20.5 kPa) using sandpaper grit P320.

Durability tests were also conducted using different grit numbers for a better understanding of the durability properties. First, to evaluate the effect of roughness on the ice adhesion of abraded surfaces, we tried to reduce the roughness of the abraded area. For this purpose, 400 cycles with sandpaper P600 (average particle diameter 26 μm), 400 cycles using sandpaper P800 (22 μm), and 400 cycles using sandpaper P1200 (15 μm) were performed. This abrasion protocol will be referred to as P1200 abrasion. Later, to increase the roughness and produce more intense wear, 600 cycles with sandpaper P60 (260 μm) were also performed.

This abrasion method is similar to the one described in other studies to evaluate the durability of icephobic materials.[43−47] An image of the test can be found in Supporting Information Figure S2.

2.4. Wear by Erosion. A homemade setup was designed to simulate prolonged wear by particle impact (erosion) at outdoor conditions. A similar strategy was proposed to determine the durability of SHSs.[48] A funnel (ENDO glassware 100 mm, 60° container angle, tube of 97 ± 1 mm, 12.00 ± 0.05 mm external diameter, 9.30 ± 0.15 mm internal diameter, 45° tube end angle) was placed over the sample at 25 ± 1 cm distance. The sample was placed on a wedge-shaped holder of 45°. The funnel hole was initially blocked, and the funnel was filled with 30 ± 1 mL (55 ± 2 g) of abrasive sand ASTM 20−30 (silicon dioxide), provided by U.S. Silica Company (Ottawa, Illinois). Then, the funnel was opened, and the sand fell on the sample (see Supporting Information Figure S2). This is a single erosion cycle.

In addition, the surfaces were also eroded by using the standard test ASTM D968, usually known as the falling sand abrasion test. This test consists in a 60° funnel connected to a cylindrical guide tube of 19.05 ± 0.08 mm (internal diameter). At the joint of the tube with the funnel, there is a metal piece that blocks the sand. The tube length is 914.4 ± 0.25 mm, and it is placed at 25.4 mm over the sample. In this case, a single erosion cycle corresponds to 3 L of falling sand. The surfaces were cleaned with a brush and rinsed with Milli-Q water or ethanol before the damage evaluation.

The weight and thickness loss as well as surface roughness were evaluated. With each erosion tests, an elliptical zone was visible. For the homemade erosion test, the width of the zone was 15 ± 1 mm, and the length was 22 ± 1 mm, so the average

damaged area was 260 ± 40 mm^2. For the D968 test, the width was 27 ± 1 mm, the length was 34 ± 1 mm, and the area was 720 ± 70 mm^2. To determine the loss in the de-icing performance, we conducted ice adhesion strength measurements after all the erosion cycles.

3. RESULTS

3.1. Surface Characterization. The different properties of the studied surfaces are collected in Table 1. The surface 1:10

Table 1. Elastic Moduli, Roughness Parameters, Ice Adhesion Strength, and Wettability Properties of the PDMS Surfaces Prepared in This Study

	surfaces		
	1:10	1:1	1:2.50%
E (MPa)	2.87 ± 0.18	2.31 ± 0.23	0.72 ± 0.03
R_a (nm)	21 ± 3	25 ± 5	19 ± 4
R_q (nm)	27 ± 4	34 ± 6	24 ± 6
SA (deg)	46.7 ± 1.3	16.4 ± 0.9	11.8 ± 0.4
ACA (deg)	126.1 ± 0.6	120.9 ± 0.9	115.9 ± 0.8
RCA (deg)	47.1 ± 1.6	87.8 ± 1.6	92.8 ± 1.0
tensile (kPa)	76 ± 8	39 ± 13	13.2 ± 2.4
shear (kPa)	70 ± 5	27 ± 3	10.8 ± 1.7

is the hardest one (higher elastic modulus), whereas the surface 1:2.50% is significantly soft. On the other hand, all the surfaces show very low surface roughness with R_a and R_q values lower than 40 nm. From the wetting properties (ACA, RCA, and SA) measured with the tilting plate, it is noticeable that the surface 1:2.50% is more hydrophobic than the rest of surfaces, presenting the lowest SA. The surface 1:1 is also hydrophobic, but the surface 1:10 has a high SA and low RCA, which is usually related with high adhesion to water.[49] All the surfaces show ice adhesion strength below 100 kPa in both tensile and shear modes. In particular, the surface 1:2.50% presents the lowest ice adhesion strength, with values around 10 kPa. This super-low adhesion is caused by low elastic modulus, hydrophobicity, and interfacial slippage.[30]

In Figure 1, we show the wetting properties measured using the growing-shrinking drop method. In this case, the relaxed RCA (measured in the quasi-static regime) is similar for the surfaces 1:10 and 1:1, but the contact angle hysteresis (CAH)
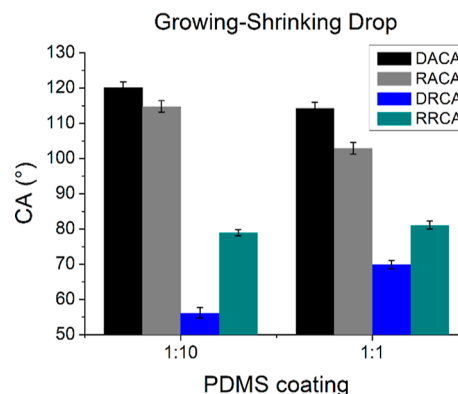
Figure 1. Wetting properties of the PDMS 1:10 and 1:1 surfaces. Black and blue bars represent dynamic (D) ACA and RCA, respectively. Gray and dark-cyan bars represent quasi-static or relaxed (R) ACA and RCA.

is still lower for the surface 1:1. This typically produces a higher water mobility.[49,50]

3.2. Evaluation of Abrasion Resistance. The core property of the surfaces fabricated in this study is their low ice adhesion. Ice adhesion strength is influenced by wetting properties (specially the RCA), elastic moduli and surface roughness.[29,51−54] For this reason, in this work, we focused on the analysis of surface durability by monitoring the ice adhesion strength. In Figure 2, we plot the ice adhesion
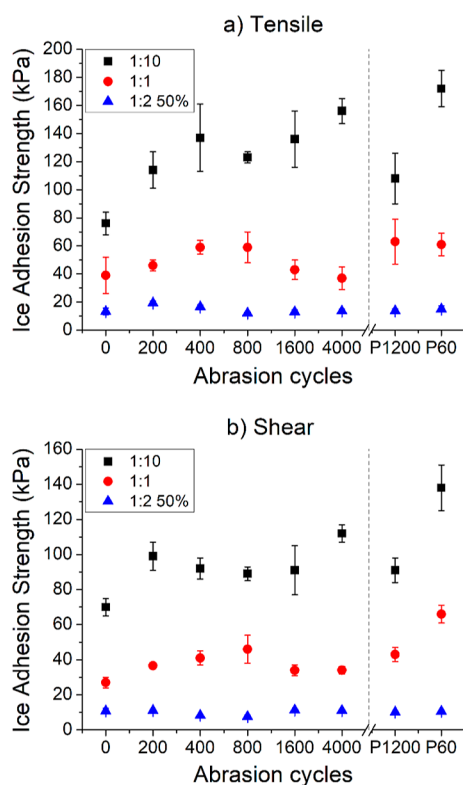
Figure 2. Ice adhesion strength in terms of abrasion cycles in (a) tensile and (b) shear modes. Ice adhesion after abrasion with high grit (P1200) and low grit (P60) is also shown. These abrasions were accumulative, so abrasion with P1200 was performed after 4000 cycles with P320 and abrasion with P60 after abrasion with P1200.

strength of the surfaces after different number of abrasion cycles using the P320 sandpaper. We noticed that for the surface 1:10, the ice adhesion in the tensile mode increased considerably up to almost twice its initial value after 4000 abrasive cycles. Similarly, the adhesion increased in the shear mode. On the other hand, the surface 1:1 initially increased its ice adhesion strength about a 50% after 800 cycles, but it decreased to their initial values after 4000 cycles. Finally, the surface 1:2.50% maintained similar values of ice adhesion strength regardless of the number of cycles.

To explore how the wear abrasion affects the ice adhesion strength, we used sandpapers of different grit numbers (see Section 2.3). In the right part of Figure 2, we can observe how ice adhesion changes as the used sandpaper. In Table 2, we summarize the roughness parameters of the surfaces after wear tests. From the results of the surface 1:10, we may conclude that roughness and ice adhesion are correlated: higher roughness, higher ice adhesion. This could be originated by an increase in actual water-surface contact area that enhanced the interlocking mechanism.[13,53,54] In our setup, it is not possible to know if the water (ice) fully penetrates on the surface roughness, so the real water-surface contact area cannot be calculated. However, even if it penetrates only partially, the real contact area must increase with respect to original surfaces, as clear from wettability results (see later in this section). However, for the surface 1:1, this interlocking effect is unclear. Otherwise, the ice adhesion on the surface 1:2.50% is not influenced by the surface roughness (no significative difference over a wide range of roughness values). This could be considered a first proof that the detachment mechanism of this surface is valid even for high surface roughness, something previously stated as a matter of study.[25] To clarify whether the ice adhesion was proportional to the roughness of the surface 1:1, we measured their roughness parameters for all number of abrasion cycles. We postulated that the peak of ice adhesion observed for the surface 1:1 (see Figure 2) was related with another peak of surface roughness. However, the expected relation between ice adhesion and surface roughness was not found (see Figure 3). The roughness reached a stable value after 400 abrasion cycles.

A clear dependence between ice adhesion and roughness was only observed for the surface 1:10, while for the surface 1:2.50%, both properties seem to be uncorrelated. Finally, the

Table 2. Roughness Parameters of the PDMS Surfaces for Different Degrees of Abrasion

|	control			after 4000 cycles P320	
50×	R_a (nm)	R_q (nm)	50×	R_a (μm)	R_q (μm)
1:10	21 ± 3	27 ± 4	1:10	3.2 ± 0.6	4.0 ± 0.8
1:1	25 ± 5	34 ± 6	1:1	3.1 ± 0.9	3.9 ± 0.9
1:2.50%	19 ± 4	24 ± 6	1:2.50%	2.8 ± 0.9	3.5 ± 1.0
	after P1200 abrasion			after P60 abrasion	
50×	R_a (μm)	R_q (μm)	50×	R_a (μm)	R_q (μm)
1:10	1.65 ± 0.11	2.07 ± 0.08	1:10	10 ± 7	12 ± 7
1:1	0.9 ± 0.3	1.2 ± 0.3	1:1	14 ± 7	18 ± 8
1:2.50%	1.14 ± 0.14	1.41 ± 0.19	1:2.50%	13 ± 3	16 ± 3
	after P60 abrasion			after P60 abrasion	
20×	R_a (μm)	R_q (μm)	10×	R_a (μm)	R_q (μm)
1:10	11 ± 3	14 ± 3	1:10	11.3 ± 0.8	16.1 ± 0.9
1:1	35 ± 19	42 ± 19	1:1	45 ± 13	56 ± 16
1:2.50%	31 ± 8	38 ± 9	1:2.50%	43 ± 11	54 ± 13
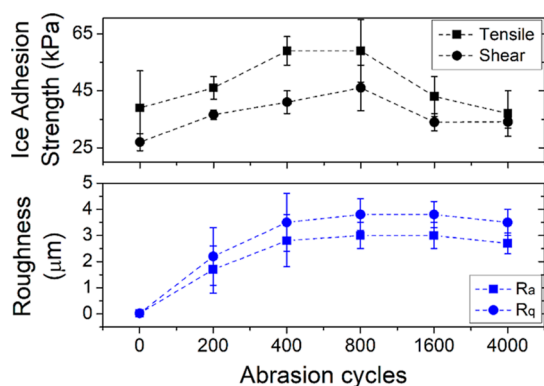
Figure 3. Roughness change for the PDMS surface 1:1 for different numbers of abrasion cycles with grit P320 compared with the ice adhesion strength change.

surface 1:1 shows a roughness—adhesion correlation only noticeable at a certain level in the shear mode, when the roughness is significantly high (after abrading with the coarse P60 sandpaper). This points out to the fact that the surfaces with low elastic moduli, such as PDMS 1:2.50%, might avoid the interlocking effect.

The abrasion with the P60 sandpaper (see Section 2.3) produced a high roughness due to its large average particle diameter (260 μm). This roughness was measured by using larger scanning areas and lower magnification (see Section 2.2.3).

In addition, we analyzed the wetting properties of the surfaces after 4000 abrasive cycles with the sandpaper P320. The results of the tilting plate experiments show an increase in the surface wettability because both the SA and CAH increase (see Figure 4). This loss of water-dislike properties may be justified by the increase in roughness: for water drops in the Wenzel state,[55] an increase in roughness leads to an increase in CAH due to the presence of anchor points that pin the contact line.[56−58] In Figure 5, we plot the water contact angles measured with the growing-shrinking drop method after abrasion. The results obtained with this method reveal the increase in CAH as well (compared with Figure 1). It is important to highlight that in both methods, tilting plate and growing-shrinking, the water contact angle measurements were carried out with drops intended to move perpendicular in the direction to the grooves created by the abrader. This was carried out to evaluate surfaces in the worst condition. On these abraded surfaces, sessile drops show a non-axisymmetric shape. Since we measured the contact angles in the surface direction that maximizes the observed CAH (see Supporting Information Figure S3), this parameter might be over-estimated.

Finally, to evaluate the durability of the PDMS surfaces more precisely, we show in Figure 6 the thickness loss, estimated from the weight loss normalized by abraded area. Here, we can observe that the material (weight) loss is more pronounced for surfaces with low elastic moduli. In addition, we may observe that the weight loss scales linearly with the number of cycles, as expected (see Supporting Information Figure S4). This observation was confirmed for the rest of the wear tests conducted with sandpapers of different grit numbers. Thus, the PDMS surface with the lowest elastic modulus and lowest ice adhesion strength revealed higher thickness loss. However, even for this case, the resistance
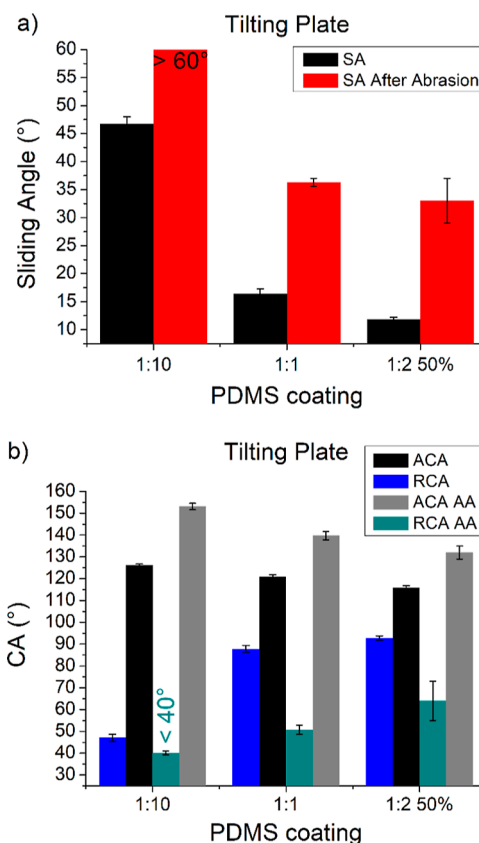

Figure 4. Wetting properties estimated by tilting plate experiments. (a) SA for the PDMS surfaces measured before and after abrasion (AA). (b) ACA and RCA for the PDMS surfaces measured before and after abrasion (AA). For the PDMS surface 1:10, SA and RCA after abrasion were greater and lower, respectively, than the represented, due to the experimental limitations (the maximum tilting angle of the device is 60°).
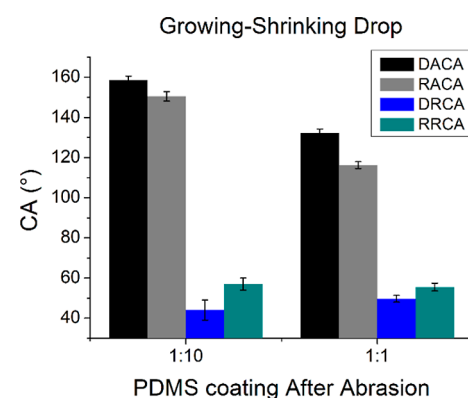
Figure 5. Wetting properties of the PDMS surfaces 1:10 and 1:1 after abrasion with P320 for 4000 cycles. Black and blue bars correspond to the dynamic (D) ACA and RCA, respectively. Gray and dark-cyan bars reflect the quasi-static or "relaxed" (R) ACA and RCA.

seems to be reasonably good. After 4000 cycles, only about 0.12 mm of thickness was lost, which points out to a large durability.

As mentioned, the ice adhesion strength values measured for the PDMS surface 1:2.50% were unaltered by the abrasion tests. Therefore, we may assume that its low ice adhesion is not only a surface property but a bulk property as well. One should expect that the coating properties will endure until no coating
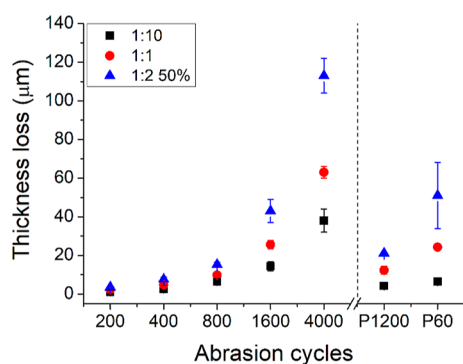
Figure 6. Thickness loss for the PDMS surfaces in terms of the number of abrasion cycles. Abrasion cycles were carried out with an abrader of grit number P320. For comparison, abrasion with other grit numbers P1200 (for smoothing) and P60 (for roughening) is also shown.

Figure 7. Dependence of thickness loss of the PDMS surfaces 1:10 in terms of the number of abrasion cycles with grit P320 and with P60 for 600 cycles (worst conditions). We varied the initial coating thickness and further studied the case of low pressure with grit P320.

is remaining, as proposed previously for these kinds of materials.[44] However, we should also take into account that on elastic surfaces, ice adhesion strength (τ) depends on thickness coating as the relation $\tau \propto \sqrt{W_a G / t}$, where W_a is the work of adhesion, G is the shear modulus, and t the coating thickness. Thus, ice adhesion increases for decreasing thicknesses.[28,29,43,52] Some studies pointed out to that, above a certain thickness, elastic coatings behave as bulk materials, and ice adhesion remains almost constant. For Beemer et al.,[43] this critical thickness is about 1400 μm, but for Wang et al.[28] and Zhuo et al.,[25] it is about 500 μm. Thus, our surface 1:2.50% presents large durability, resisting at least 25,000 abrasion cycles with P320 before noticeably increasing the ice adhesion strength. With respect to the rest of the surfaces studied here, they show larger durability in terms of coating thickness. However, the surface 1:10 increases its ice adhesion values after abrasion (probably due to a roughness increase), whereas the surface 1:1 shows a wide range of ice adhesion values after abrasion, including a certain increase with respect to the initial values, even though they are not necessarily related with roughness.

We found that the PDMS surfaces are more resistant to abrasion (lower coating thickness loss) than ductile non-elastic materials (paraffin) and similar to the aluminum surfaces (see Supporting Information Section S4). This could be due to the ability of elastic materials to be deformed without breaking. A clear example is found in ref 59 where a saw easily cut hard materials, but it is not able to cut deformable materials, unless they are fully fixed. Somehow, elastic surfaces accommodate to the abrader minimizing the mass removal. Following this hypothesis, one might call into question whether abrasion will produce the same weight loss regardless of the thickness. Due to its lower thickness, the PDMS coating is less mobile under the abradant pressure, and consequently, it could be more easily abraded. To illustrate this issue, in Figure 7, we plot the thickness loss for the surface 1:10 with different coating thicknesses. In addition, we also evaluated durability under lower pressure. We found that the weight loss during surface abrasion is almost independent of the coating thickness, at least for coating thicknesses above 280 μm. In fact, the mass removal was lower for thinner coating when we used the sandpaper P320, while the opposite trend happened with P60. In conclusion, the current coating thickness does not seem to affect the wear rate, while the properties of the abrader seem to
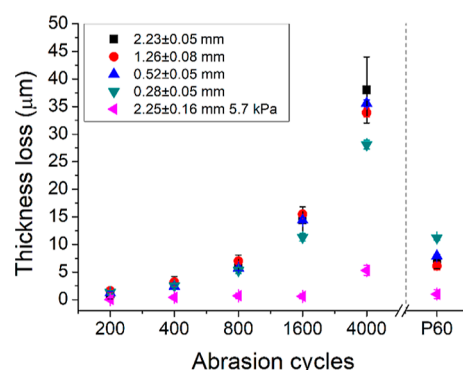
play a more important role. In any case, the surface durability under abrasion seems to be independent of thickness over a wide range of values. In consequence, the durability of the PDMS coating will only depend on its initial thickness.

3.3. Evaluation of Resistance to Erosion. To evaluate the wear induced by particle impact (erosion), we measured the roughness parameters and thickness losses. We also evaluated ice adhesion once the full erosion test was performed. In Figure 8, we plot the apparent thickness loss
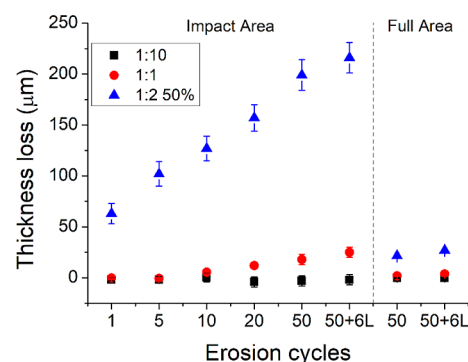
Figure 8. Thickness loss produced by the sand test for the different PDMS surfaces in terms of erosion cycles. Thickness loss was calculated from the attacked zone and all the sample area. Notice that the erosion with the ASTM D968 setup was performed after total erosion conducted with the ad hoc test. Thus, the weight loss reflects the first 50 cycles and the two cycles (D968 setup) together, denoted as "50+6L."

of the three different coatings for different numbers of erosion cycles with a homemade setup (see Section 2.4 for details). We also included the final test with the ASTM D968 setup. As mentioned in the previous section, we evaluated the thickness loss as the ratio between weight loss by eroded area. According to the results shown in Figure 8, the thickness loss for the surfaces 1:10 and 1:1 was very low. However, the surface 1:2.50% was significantly damaged after these tests. The wear induced by erosion for this kind of samples was even greater than the one observed for the linear abrasion test. However, the thickness loss does not scale linearly with the number of cycles. As can be seen in Supporting Information Section S5, this is due to the fact that sand impact is not the unique source of surface wearing. We found a direct evidence that a remarkable part of the damage was produced by removing

the sand from the samples between different erosion cycles. We observed that the sand stuck to the PDMS surface, especially on the softest one. During the cleaning process, the sand detached from the surface may enhance the mass loss by cohesive failure. Consequently, we argue that the thickness loss may be calculated by using the full area, not only the apparent damaged area (sand impact zone). Thus, we also included in Figure 8 the thickness loss calculated using the full area. With this approximation, the calculated thickness loss is very low for the three surfaces, as expected.

To validate the apparent resistance of PDMS coatings to erosion, it is necessary to check out how the ice adhesion strength is affected after wear tests. Results can be found in Table 3. After the erosion cycles, most surfaces maintained

Table 3. Ice Adhesion Strength After the Falling Sand Test

	surfaces		
ice adhesion strength	1:10	1:1	1:2.50%
tensile (kPa)	88 ± 16	52 ± 6	11.0 ± 2.2
shear (kPa)	89 ± 8	31 ± 4	10.1 ± 1.4
Original Values			
tensile (kPa)	76 ± 8	39 ± 13	13.2 ± 2.4
shear (kPa)	70 ± 5	27 ± 3	10.8 ± 1.7

their low ice adhesion properties, compared to the control samples, within the experimental error. The surfaces 1:10 presented the most noticeable variation with respect to the control surfaces. However, since this surface neither revealed important mass loss nor roughness increase, the increase in ice adhesion strength could only be attributed to the intrinsic variability between different replicas. Thus, we conclude that the PDMS surfaces maintain their low ice adhesion properties and present considerable durability under erosion tests.

For comparison, the values for control surfaces from Table 1 are also shown.

4. DISCUSSION

In this study, we explored the durability properties of several soft coatings with low ice adhesion properties. The durability was studied by analyzing how the wear tests modified the ice adhesion properties of the coatings. Our results are in overall satisfactory, in comparison with previous studies. For example, Beemer et al.[43] presented PDMS gels that maintain their properties after more than 1000 abrasion cycles by using a setup similar to this study, with similar grit number of the abrader (sandpaper grit 400) but lower pressure (6.8 kPa). Similarly, Zhuo et al.[45] studied durability of their anti-icing materials by applying 1.5 kPa and grit number 400. In the present work, the used pressure was higher (20.5 kPa), and as shown in Figure 7, the wear tests conducted with lower pressure (about 5.7 kPa) provided much lower thickness loss. In addition, we found that the surface 1:2.50% maintained low ice adhesion, showing no evidence of the interlocking effect. This phenomenon is usually assumed as the origin of the ice adhesion increase observed after conducting the wearing tests.[43,45] In conclusion, our surfaces showed better durability than other proposed solutions because they resisted more cycles and under higher pressure. We further estimated the resistance of our coatings through the thickness loss, resulting in large durability.

On the other hand, we found that erosion did not have a strong impact on the samples. Nevertheless, we found that the

dirt that was accumulated on surfaces during the erosion tests was hardly cleanable. Indeed, we observed that some dirt remained attached after the cleaning process (see Supporting Information Section S6). This might be a problem in real applications because the fabricated surfaces may accumulate environmental dirt. However, we found that the ice adhesion strength remains low, almost unaltered, for the three kinds of surfaces. Thus, the anti-icing performance of these surfaces is not much affected by erosion.

In comparison to other harder coatings proposed in the literature (such as aluminum coated with a thin film of fluoropolymer[60]), which lose their wettability properties and consequently the icephobic properties after few wear cycles,[42] the PDMS elastic materials proposed in this work are able to maintain the icephobic properties after highly aggressive wear tests. This is a proof of the advantage that is added when using coatings whose bulk properties instead of surface properties are relevant.[48]

However, in our opinion, to compare meaningfully surface resistance and durability the conditions should be harsher, such as higher pressure or more abrasive agents (like P60 sandpaper). Other studies have examined durability under "presumably" higher pressures,[44,46] but none of these studies specified the pressure value, only the load applied. We explored the durability under higher pressure, and we found that the surface 1:2.50% was destroyed after 120 cycles at 110 kPa, while the other two surfaces resisted the abrasion (see Supporting Information Figure S8). Thus, the surface 1:2.50% does not tolerate high pressure in abrasion. It would be important to estimate the actual magnitude of abrasion that working surfaces suffer under real conditions.

We evaluated the resistance under abrasion and erosion, but there are other types of damage in real world. For example, less cross-linked PDMS (far from the 1:10 ratio) reveals lower E and lower resistance to break under tension (ultimate tensile strength) but higher maximum elongation.[61] In consequence, although in our study, we report a great mechanical durability of PDMS surfaces, they could be weak under other stresses. For this reason, a more complete evaluation would be necessary to establish the practical durability.

5. CONCLUSIONS

We examined the durability properties of three types of PDMS-based elastic surfaces under abrasion and erosion, in terms of ice adhesion, thickness loss, and roughness modification. We found that, due to their deformability, these surfaces resist abrasion reasonably well, maintaining a low ice adhesion strength after more than 4000 abrasion cycles. The icephobic performance is preserved until the coating thickness is low enough to influence ice adhesion. We found that the low ice adhesion values of the surfaces fabricated in this study are more likely attributed to the bulk property rather than surface response. The elastic coating preserved its properties although it was partly damaged. For this reason, the interlocking effect seems to be absent in elastic surfaces above an elasticity degree. On the other hand, we found that the surfaces become more wettable due to roughness increase.

We also evaluated the resistance of the surfaces to erosion, and we found that the erosion was low for most surfaces, especially those ones with higher elastic modulus. In general, the thickness loss was low, and the ice adhesion strength maintained low values. In our wear experiments, the softest surface presented the fastest decrease in coating thickness,

although its ice adhesion strength was unmodified, being the lowest ice adhesion strength.

In conclusion, moderate elastic surfaces presented good durability although their adhesion strength increased upon accumulating wear agents. Otherwise, the softest elastic surface presented the best results of durability although their suitability for real applications would require further studies conducted under more realistic conditions.

■ ASSOCIATED CONTENT

Ⓢⓘ Supporting Information

The Supporting Information is available free of charge at https://pubs.acs.org/doi/10.1021/acsomega.2c01134.

> Detailed explanation of the durability characterization (PDF)

■ AUTHOR INFORMATION

Corresponding Author

Miguel A. Rodríguez-Valverde − *Laboratory of Surface and Interface Physics, Department of Applied Physics, University of Granada, ES-18071 Granada, Spain;* ⓞ orcid.org/0000-0003-4361-6721; Email: marodri@ugr.es

Authors

Pablo F. Ibáñez-Ibáñez − *Laboratory of Surface and Interface Physics, Department of Applied Physics, University of Granada, ES-18071 Granada, Spain;* ⓞ orcid.org/0000-0001-6479-7029

Francisco Javier Montes Ruiz-Cabello − *Laboratory of Surface and Interface Physics, Department of Applied Physics, University of Granada, ES-18071 Granada, Spain*

Miguel A. Cabrerizo-Vílchez − *Laboratory of Surface and Interface Physics, Department of Applied Physics, University of Granada, ES-18071 Granada, Spain*

Complete contact information is available at:
https://pubs.acs.org/10.1021/acsomega.2c01134

Author Contributions

P.F.I.-I.: Conceptualization, investigation, methodology, formal analysis, visualization, and writing—original draft. F.J.M.R.-C.: Conceptualization, writing—review, editing, and supervision. M.A.C.-V.: Resources, funding acquisition, and project administration. M.A.R.-V.: Conceptualization, writing—review, editing, supervision, funding acquisition, and project administration.

Notes

The authors declare no competing financial interest.

■ ACKNOWLEDGMENTS

■ REFERENCES

(1) Mishchenko, L.; Hatton, B.; Bahadur, V.; Taylor, J. A.; Krupenkin, T.; Aizenberg, J. Design of Ice-Free Nanostructured Surfaces Based on Repulsion of Impacting Water Droplets. *ACS Nano* **2010**, *4*, 7699−7707.

(2) Maitra, T.; Antonini, C.; Tiwari, M. K.; Mularczyk, A.; Imeri, Z.; Schoch, P.; Poulikakos, D. Supercooled Water Drops Impacting Superhydrophobic Textures. *Langmuir* **2014**, *30*, 10855−10861.

(3) Li, J.; Luo, Y.; Zhu, J.; Li, H.; Gao, X. Subcooled-Water Nonstickiness of Condensate Microdrop Self-Propelling Nanosurfaces. *ACS Appl. Mater. Interfaces* **2015**, *7*, 26391−26395.

(4) Zhang, R.; Hao, P.; Zhang, X.; He, F. Supercooled Water Droplet Impact on Superhydrophobic Surfaces with Various Roughness and Temperature. *Int. J. Heat Mass Transfer* **2018**, *122*, 395−402.

(5) Boinovich, L.; Emelyanenko, A. M.; Korolev, V. V.; Pashinin, A. S. Effect of Wettability on Sessile Drop Freezing: When Superhydrophobicity Stimulates an Extreme Freezing Delay. *Langmuir* **2014**, *30*, 1659−1668.

(6) Liu, Y.; Li, X.; Jin, J.; Liu, J.; Yan, Y.; Han, Z.; Ren, L. Anti-Icing Property of Bio-Inspired Micro-Structure Superhydrophobic Surfaces and Heat Transfer Model. *Appl. Surf. Sci.* **2017**, *400*, 498−505.

(7) Wen, M.; Wang, L.; Zhang, M.; Jiang, L.; Zheng, Y. Antifogging and Icing-Delay Properties of Composite Micro- and Nanostructured Surfaces. *ACS Appl. Mater. Interfaces* **2014**, *6*, 3963−3968.

(8) Hao, Q.; Pang, Y.; Zhao, Y.; Zhang, J.; Feng, J.; Yao, S. Mechanism of Delayed Frost Growth on Superhydrophobic Surfaces with Jumping Condensates: More than Interdrop Freezing. *Langmuir* **2014**, *30*, 15416−15422.

(9) Chen, J.; Liu, J.; He, M.; Li, K.; Cui, D.; Zhang, Q.; Zeng, X.; Zhang, Y.; Wang, J.; Song, Y. Superhydrophobic Surfaces Cannot Reduce Ice Adhesion. *Appl. Phys. Lett.* **2012**, *101*, 111603.

(10) Varanasi, K. K.; Deng, T.; Smith, J. D.; Hsu, M.; Bhate, N. Frost Formation and Ice Adhesion on Superhydrophobic Surfaces. *Appl. Phys. Lett.* **2010**, *97*, 234102.

(11) Liu, Y.; Choi, C.-H. Condensation-Induced Wetting State and Contact Angle Hysteresis on Superhydrophobic Lotus Leaves. *Colloid Polym. Sci.* **2013**, *291*, 437−445.

(12) Farhadi, S.; Farzaneh, M.; Kulinich, S. A. Anti-Icing Performance of Superhydrophobic Surfaces. *Appl. Surf. Sci.* **2011**, *257*, 6264−6269.

(13) Kulinich, S. A.; Farhadi, S.; Nose, K.; Du, X. W. Superhydrophobic Surfaces: Are They Really Ice-Repellent? *Langmuir* **2011**, *27*, 25−29.

(14) Yu, D. I.; Doh, S. W.; Kwak, H. J.; Kang, H. C.; Ahn, H. S.; Park, H. S.; Kiyofumi, M.; Kim, M. H. Wetting State on Hydrophilic and Hydrophobic Micro-Textured Surfaces: Thermodynamic Analysis and X-Ray Visualization. *Appl. Phys. Lett.* **2015**, *106*, 171602.

(15) Nagayama, G.; Zhang, D. Intermediate Wetting State at Nano/Microstructured Surfaces. *Soft Matter* **2020**, *16*, 3514−3521.

(16) Wong, T.-S.; Kang, S. H.; Tang, S. K. Y.; Smythe, E. J.; Hatton, B. D.; Grinthal, A.; Aizenberg, J. Bioinspired Self-Repairing Slippery Surfaces with Pressure-Stable Omniphobicity. *Nature* **2011**, *477*, 443−447.

(17) Kim, P.; Wong, T.-S.; Alvarenga, J.; Kreder, M. J.; Adorno-Martinez, W. E.; Aizenberg, J. Liquid-Infused Nanostructured Surfaces with Extreme Anti-Ice and Anti-Frost Performance. *ACS Nano* **2012**, *6*, 6569−6577.

(18) Chen, X.; Wen, G.; Guo, Z. What Are the Design Principles, from the Choice of Lubricants and Structures to the Preparation Method, for a Stable Slippery Lubricant-Infused Porous Surface? *Mater. Horiz.* **2020**, *7*, 1697−1726.

(19) Rykaczewski, K.; Anand, S.; Subramanyam, S. B.; Varanasi, K. K. Mechanism of Frost Formation on Lubricant-Impregnated Surfaces. *Langmuir* **2013**, *29*, 5230−5238.

(20) Erbil, H. Y. Improvement of Lubricant-Infused Surfaces for Anti-Icing Applications. *Surf. Innov.* **2016**, *4*, 214−217.

(21) Ozbay, S.; Yuceel, C.; Erbil, H. Y. Improved Icephobic Properties on Surfaces with a Hydrophilic Lubricating Liquid. *ACS Appl. Mater. Interfaces* **2015**, *7*, 22067−22077.

(22) Smith, J. D.; Dhiman, R.; Anand, S.; Reza-Garduno, E.; Cohen, R. E.; McKinley, G. H.; Varanasi, K. K. Droplet Mobility on Lubricant-Impregnated Surfaces. *Soft Matter* **2013**, *9*, 1772−1780.

(23) Sett, S.; Yan, X.; Barac, G.; Bolton, L. W.; Miljkovic, N. Lubricant-Infused Surfaces for Low-Surface-Tension Fluids: Promise versus Reality. *ACS Appl. Mater. Interfaces* **2017**, *9*, 36400−36408.

(24) Wang, J.; Kato, K.; Blois, A. P.; Wong, T.-S. Bioinspired Omniphobic Coatings with a Thermal Self-Repair Function on Industrial Materials. *ACS Appl. Mater. Interfaces* **2016**, *8*, 8265−8271.

(25) Zhuo, Y.; Xiao, S.; Amirfazli, A.; He, J.; Zhang, Z. Polysiloxane as Icephobic Materials − The Past, Present and the Future. *Chem. Eng. J.* **2021**, *405*, 127088.

(26) Kreder, M. J.; Alvarenga, J.; Kim, P.; Aizenberg, J. Design of Anti-Icing Surfaces: Smooth, Textured or Slippery? *Nat. Rev. Mater.* **2016**, *1*, 1−15.

(27) He, Z.; Xiao, S.; Gao, H.; He, J.; Zhang, Z. Multiscale Crack Initiator Promoted Super-Low Ice Adhesion Surfaces. *Soft Matter* **2017**, *13*, 6562−6568.

(28) Wang, C.; Fuller, T.; Zhang, W.; Wynne, K. J. Thickness Dependence of Ice Removal Stress for a Polydimethylsiloxane Nanocomposite: Sylgard 184. *Langmuir* **2014**, *30*, 12819−12826.

(29) He, Z.; Zhuo, Y.; He, J.; Zhang, Z. Design and Preparation of Sandwich-like Polydimethylsiloxane (PDMS) Sponges with Super-Low Ice Adhesion. *Soft Matter* **2018**, *14*, 4846−4851.

(30) Ibáñez-Ibáñez, P. F.; Montes Ruiz-Cabello, F. J.; Cabrerizo-Vílchez, M. A.; Rodríguez-Valverde, M. A. Ice Adhesion of PDMS Surfaces with Balanced Elastic and Water-Repellent Properties. *J. Colloid Interface Sci.* **2022**, *608*, 792−799.

(31) Zhu, L.; Xue, J.; Wang, Y.; Chen, Q.; Ding, J.; Wang, Q. Ice-Phobic Coatings Based on Silicon-Oil-Infused Polydimethylsiloxane. *ACS Appl. Mater. Interfaces* **2013**, *5*, 4053−4062.

(32) Yeong, Y. H.; Wang, C.; Wynne, K. J.; Gupta, M. C. Oil-Infused Superhydrophobic Silicone Material for Low Ice Adhesion with Long-Term Infusion Stability. *ACS Appl. Mater. Interfaces* **2016**, *8*, 32050−32059.

(33) Zhuo, Y.; Wang, F.; Xiao, S.; He, J.; Zhang, Z. One-Step Fabrication of Bioinspired Lubricant-Regenerable Icephobic Slippery Liquid-Infused Porous Surfaces. *ACS Omega* **2018**, *3*, 10139−10144.

(34) Zhao, H.; Sun, Q.; Deng, X.; Cui, J. Earthworm-Inspired Rough Polymer Coatings with Self-Replenishing Lubrication for Adaptive Friction-Reduction and Antifouling Surfaces. *Adv. Mater.* **2018**, *30*, 1802141.

(35) Zhuo, Y.; Håkonsen, V.; He, Z.; Xiao, S.; He, J.; Zhang, Z. Enhancing the Mechanical Durability of Icephobic Surfaces by Introducing Autonomous Self-Healing Function. *ACS Appl. Mater. Interfaces* **2018**, *10*, 11972−11978.

(36) Pierce, E.; Carmona, F. J.; Amirfazli, A. Understanding of Sliding and Contact Angle Results in Tilted Plate Experiments. *Colloids Surf., A* **2008**, *323*, 73−82.

(37) Ruiz-Cabello, F. J. M.; Rodríguez-Valverde, M. A.; Cabrerizo-Vílchez, M. A New Method for Evaluating the Most Stable Contact Angle Using Tilting Plate Experiments. *Soft Matter* **2011**, *7*, 10457−10461.

(38) Extrand, C. W.; Kumagai, Y. An Experimental Study of Contact Angle Hysteresis. *J. Colloid Interface Sci.* **1997**, *191*, 378−383.

(39) Moraila-Martínez, C. L.; Montes Ruiz-Cabello, F. J.; Cabrerizo-Vílchez, M. A.; Rodríguez-Valverde, M. A. The Effect of Contact Line Dynamics and Drop Formation on Measured Values of Receding Contact Angle at Very Low Capillary Numbers. *Colloids Surf., A* **2012**, *404*, 63−69.

(40) Kwok, D. Y.; Lin, R.; Mui, M.; Neumann, A. W. Low-Rate Dynamic and Static Contact Angles and the Determination of Solid Surface Tensions. *Colloids Surf., A* **1996**, *116*, 63−77.

(41) Ibáñez-Ibáñez, P. F.; Montes Ruiz-Cabello, F. J.; Cabrerizo-Vílchez, M. A.; Rodríguez-Valverde, M. A. Contact Line Relaxation of Sessile Drops on PDMS Surfaces: A Methodological Perspective. *J. Colloid Interface Sci.* **2021**, *589*, 166−172.

(42) Montes Ruiz-Cabello, F. J.; Ibañez-Ibáñez, P.; Paz-Gomez, G.; Cabrerizo-Vilchez, M.; Rodriguez-Valverde, M. A. Fabrication of Superhydrophobic Metal Surfaces for Anti-Icing Applications. *J. Visualized Exp.* **2018**, *138*, No. e57635.

(43) Beemer, D. L.; Wang, W.; Kota, A. K. Durable Gels with Ultra-Low Adhesion to Ice. *J. Mater. Chem. A* **2016**, *4*, 18253−18258.

(44) Golovin, K.; Kobaku, S. P. R.; Lee, D. H.; DiLoreto, E. T.; Mabry, J. M.; Tuteja, A. Designing Durable Icephobic Surfaces. *Sci. Adv.* **2016**, *2*, No. e1501496.

(45) Zhuo, Y.; Li, T.; Wang, F.; Håkonsen, V.; Xiao, S.; He, J.; Zhang, Z. An Ultra-Durable Icephobic Coating by a Molecular Pulley. *Soft Matter* **2019**, *15*, 3607−3611.

(46) Irajizad, P.; Al-Bayati, A.; Eslami, B.; Shafquat, T.; Nazari, M.; Jafari, P.; Kashyap, V.; Masoudi, A.; Araya, D.; Ghasemi, H. Stress-Localized Durable Icephobic Surfaces. *Mater. Horiz.* **2019**, *6*, 758−766.

(47) Yeong, Y. H.; Milionis, A.; Loth, E.; Sokhey, J. Self-Lubricating Icephobic Elastomer Coating (SLIC) for Ultralow Ice Adhesion with Enhanced Durability. *Cold Reg. Sci. Technol.* **2018**, *148*, 29−37.

(48) Milionis, A.; Loth, E.; Bayer, I. S. Recent Advances in the Mechanical Durability of Superhydrophobic Materials. *Adv. Colloid Interface Sci.* **2016**, *229*, 57−79.

(49) Gao, L.; McCarthy, T. J. Teflon Is Hydrophilic. Comments on Definitions of Hydrophobic, Shear versus Tensile Hydrophobicity, and Wettability Characterization. *Langmuir* **2008**, *24*, 9183−9188.

(50) Furmidge, C. G. L. Studies at Phase Interfaces. I. The Sliding of Liquid Drops on Solid Surfaces and a Theory for Spray Retention. *J. Colloid Sci.* **1962**, *17*, 309−324.

(51) Meuler, A. J.; Smith, J. D.; Varanasi, K. K.; Mabry, J. M.; McKinley, G. H.; Cohen, R. E. Relationships between Water Wettability and Ice Adhesion. *ACS Appl. Mater. Interfaces* **2010**, *2*, 3100−3110.

(52) Irajizad, P.; Nazifi, S.; Ghasemi, H. Icephobic Surfaces: Definition and Figures of Merit. *Adv. Colloid Interface Sci.* **2019**, *269*, 203−218.

(53) Zou, M.; Beckford, S.; Wei, R.; Ellis, C.; Hatton, G.; Miller, M. A. Effects of Surface Roughness and Energy on Ice Adhesion Strength. *Appl. Surf. Sci.* **2011**, *257*, 3786−3792.

(54) Fu, Q.; Wu, X.; Kumar, D.; Ho, J. W. C.; Kanhere, P. D.; Srikanth, N.; Liu, E.; Wilson, P.; Chen, Z. Development of Sol-Gel Icephobic Coatings: Effect of Surface Roughness and Surface Energy. *ACS Appl. Mater. Interfaces* **2014**, *6*, 20685−20692.

(55) Wenzel, R. N. Resistance of Solid Surfaces to Wetting by Water. *Ind. Eng. Chem.* **1936**, *28*, 988−994.

(56) Eral, H. B.; 't Mannetje, D. J. C. M.; Oh, J. M. Contact Angle Hysteresis: A Review of Fundamentals and Applications. *Colloid Polym. Sci.* **2013**, *291*, 247−260.

(57) Shuttleworth, R.; Bailey, G. L. J. The Spreading of a Liquid over a Rough Solid. *Discuss. Faraday Soc.* **1948**, *3*, 16−22.

(58) Meiron, T. S.; Marmur, A.; Saguy, I. S. Contact Angle Measurement on Rough Surfaces. *J. Colloid Interface Sci.* **2004**, *274*, 637−644.

(59) Halanski, M. A. How to Avoid Cast Saw Complications. *J. Pediatr. Orthop.* **2016**, *36*, S1−S5.

(60) Ruiz-Cabello, F. J. M.; Ibáñez-Ibáñez, P. F.; Gómez-Lopera, J. F.; Martínez-Aroza, J.; Cabrerizo-Vílchez, M.; Rodríguez-Valverde, M. A. Testing the Performance of Superhydrophobic Aluminum Surfaces. *J. Colloid Interface Sci.* **2017**, *508*, 129−136.

(61) Vaicekauskaite, J.; Mazurek, P.; Vudayagiri, S.; Skov, A. L. Mapping the Mechanical and Electrical Properties of Commercial Silicone Elastomer Formulations for Stretchable Transducers. *J. Mater. Chem. C* **2020**, *8*, 1273−1279.